An efficient local fundamental-mode cutoff for thermo-optic tunable Er^{3+}-doped fiber ring laser

Nan-Kuang Chen

Department of Photonics & Institute of Electro-Optical Engineering, National Chiao Tung University, Hsinchu, Taiwan 300, R.O.C
nkchen.eo90g@nctu.edu.tw

Sien Chi[*,†]

[*]*Department of Photonics & Institute of Electro-Optical Engineering, National Chiao Tung University, Hsinchu, Taiwan 300, R.O.C*
[†]*Department of Electrical Engineering, Yuan Ze University, Chungli, Taiwan 320, R.O.C*

Shiao-Min Tseng

Department of Electrical Engineering, National Tsing Hua University, Hsinchu, Taiwan 300, R.O.C

Abstract: We demonstrate a continuously tunable Er^{3+}-doped fiber laser by incorporating a short-pass filter, which provides a wideband tunable fundamental-mode cutoff with high rejection efficiency (> 45 dB/cm) at long wavelengths, into a ring resonator. The tunable short-pass filter locally suppresses the gain profile of the Er^{3+}-doped fiber at long wavelengths and makes the lasing wavelength continuously move toward short wavelengths when optical polymer is cooling down. The tuning efficiency, tuning range, signal-ASE-ratio, and FWHM linewidth of the laser are 7.65 nm/°C, 26 nm (1569.8 ~ 1595.8 nm), 40 dB, and 0.5 nm, respectively.

©2005 Optical Society of America

OCIS codes: (060.2410) Fibers, erbium; (140.3560) Lasers, ring; (160.6840) Thermo-optical materials; (240.7040) Tunneling; (999.9999) Fundamental-mode cutoff

References and links

1. D. A. Smith, M. W. Maeda, J. J. Johnson, J. S. Patel, M. A. Saifi, and A. Von Lehman, "Acoustically tuned erbium-doped fiber ring laser," Opt. Lett. **16**, 387-389 (1991).
2. Y. W. Song, S. A. Havstad, D. Starodubov, Y. Xie A. E. Willner, J. Feinberg, "40-nm-wide tunable fiber ring laser with single-mode operation using a highly stretchable FBG," IEEE Photonics Technol. Lett. **13**, 1167-1169 (2001).
3. B. O. Guan, H. Y. Tam, H. L. W. Chan, X. Y. Dong, C. L. Loong, M. S. Demokan, "Temperature-tuned erbium-doped fiber ring laser with polymer-coated fiber grating," Opt. Commun. **202**, 331-334 (2002).
4. S. Yamashita and M. Nishihara, "Widely tunable erbium-doped fiber ring laser covering both C-band and L-band," IEEE J. Sel. Top. Quantum Electron. **7**, 41-43 (2001).
5. K. R. Sohn and J. W. Song, "Thermooptically tunable side-polished fiber comb filter and its application," IEEE Photonics Technol. Lett. **14**, 1575-1577 (2002).
6. K. R. Sohn and K. Taek, "Multiwavelength all-fiber ring laser using side-polished fiber comb filter and mechanically formed long-period fiber gratings," IEEE Photonics Technol. Lett. **17**, 309-311 (2005).
7. A. Gloag, N. Langford, K. McCallion, and W. Johnstone, "Tunable, single frequency erbium fiber laser using an overlay bandpass filter," Appl. Phys. Lett. **66**, 3263-3265 (1995).
8. A. Gloag, N. Langford, K. McCallion, and W. Johnstone, "Tunable erbium fiber laser using a overlay bandpass filter," Opt. Lett. **19**, 801-803 (1994).
9. M. A. Arbore, "Application of fundamental-mode cutoff for novel amplifiers and lasers," in *Proceedings of Optical Fiber Communication Conference OFC'05 (Optical Society of America, Washi*ngton, D.C., 2005), paper OFB4.
10. M. A. Arbore, Y. Zhou, H. Thiele, J. Bromage, and L. Nelson, "S-band erbium-doped fiber amplifiers for WDM transmission between 1488 and 1508 nm," in *Proceedings of Optical Fiber Communication Conference OFC'03 (Optical Society of America, Washington, D.C., 2003)*, paper WK2.

11. M. Monerie, "Propagation in doubly clad single-mode fibers," IEEE J. Quantum Electron. **QE-18**, 535-542 (1982).

12. N. K. Chen, S. Chi, and S. M. Tseng, "Wideband tunable fiber short-pass filter based on side-polished fiber with dispersive polymer overlay," Opt. Lett. **29**, 2219-2221 (2004).

13. K. Morishita, "Bandpass and band-rejection filters using dispersive fibers," J. Lightwave Technol. **7**, 816-819 (1989).

1. Introduction

Tunable fiber lasers are essential for the fiber-optic communications and sensing. The wavelength tuning range mainly depends on the gain bandwidth of the active medium and the tuning range of the filter. Both of the Raman and Er^{3+}-doped fiber amplifiers (EDFAs) can provide a very wide gain bandwidth of up to 100 nm and, for EDFAs, the laser amplification can occur at S- (1480 ~ 1520 nm) or C- (1530 ~ 1565 nm) or L- (1570 ~ 1610 nm) bands contingent upon the erbium ion concentration, length of the erbium-doped fiber (EDF) and/or amplified spontaneous emission (ASE) suppressing filter. Tunable Er^{3+}-doped fiber lasers had been demonstrated using variant kinds of tunable filters [1-9]. Among them, the fundamental-mode cutoff wavelength (LP_{01}-λ_c) induced from a depressed inner cladding is distinguished for wideband distributed ASE suppression and was employed to achieve tunable S-band EDFAs and fiber lasers [9,10]. The depressed inner cladding in EDF modifies the waveguide dispersion, which varies the refractive index dispersion (RID) $n(\lambda)$ curves, and the effective indices of the long and short wavelengths become lower and higher than the index of the outer silica cladding, respectively [11]. The ASE peak wavelength and the longer wavelengths are substantially suppressed while the short wavelengths in S-band can thus obtain higher population inversions and sufficient amplification. The cutoff wavelength can be tuned by bending the fiber and the total distributed loss for wavelengths longer than the cutoff is > 200 dB through entire 15-m-long EDF [10]. However, the LP_{01}-λ_c induced from waveguide dispersion is only mechanically tunable and the distributed loss can only be generated at long-wavelength side of the cutoff, which is difficult to achieve tunable L-band EDFAs.
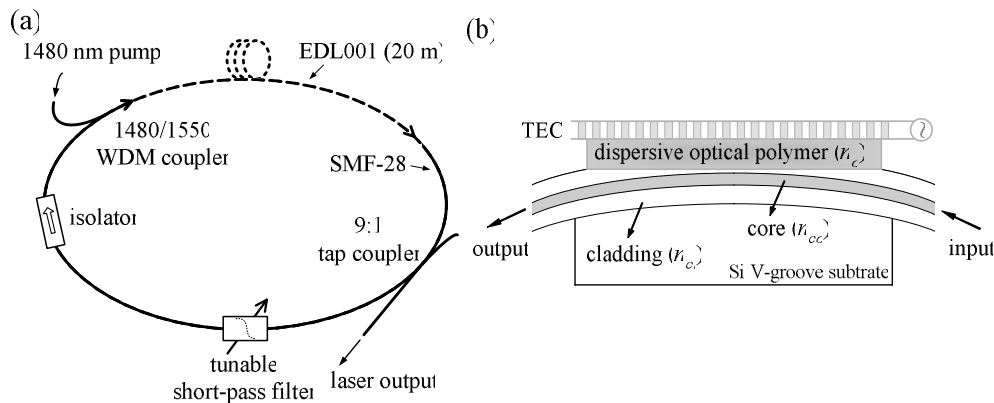

Fig. 1. (a) Experimental set up of the EDFRL and (b) Device structure of the side-polished fiber tunable short-pass filter.

In this work, we demonstrate a high-efficiency and continuously tunable Er^{3+}-doped fiber ring laser (EDFRL) with 26 nm tuning range and 40 dB signal-ASE-ratio based on a local LP_{01}-λ_c induced from material dispersion in the ring resonator shown in Fig. 1(a). The LP_{01}-λ_c is thermo-optically tunable and is obtained by overlaying the side-polished fiber (SPF) with dispersive optical polymer [12] shown in Fig. 1(b). When the dispersion slopes |dn/dλ| of the optical polymer and SPF are different, the $n(\lambda)$ curves can intersect at a LP_{01}-λ_c point which separates the wavelengths into bound and tunneling leaky modes to act as a wavelength filter. While the |dn/dλ| of the SPF is steeper than that of the optical polymer, the filter will function

as a short-pass filter [12]. On the contrary, the filter operates as a long-pass filter. A band-rejection or a band-pass filter [13] can also be obtained based on such kind of material dispersion discrepancy. The refractive index of the optical polymer changes with temperature and the LP_{01}-λ_c wavelength moves accordingly. The cross angle between the $n(\lambda)$ curves is crucial to the sharpness of the cutoff, which is related to the linewidth of the fiber laser, and the thermo-optic coefficient dn_D/dT is decisive to the temperature tuning ramp. Although SPFs had been used as filters in EDFRL [5-8], this is the first time that a side-polished short-pass filter, which provides a wideband tunable (> 400 nm) loss window with high rejection efficiency (> 45 dB/cm) for wavelengths longer than the cutoff and high tuning efficiency (26.7 nm/°C), is used to investigate the EDFRL with lasing wavelength tuning toward the shorter wavelengths through an efficient local ASE suppression in the resonator. It reflects that, based on such material dispersion discrepancy, tunable fiber short/long-pass or band-rejection filters could be employed to achieve tunable EDFAs and lasers covering S-, C-, and/or L-bands using variant optical polymers in the future.

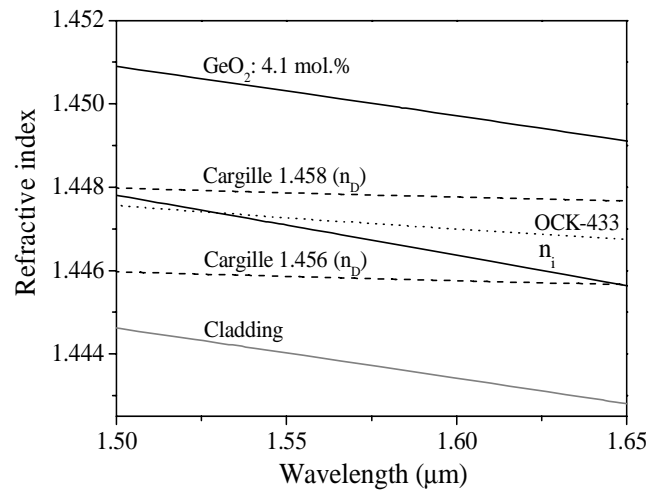## 2. Fabrication and experiments

Fig. 2. Refractive index dispersions of the fiber, Cargille index liquids and thermo-optic polymer OCK-433.

For a high efficient local ASE suppression in EDFRL, a sharp filter edge and deep stopband are required for the tunable LP_{01}-λ_c induced from material dispersion. Fig. 2 shows the RID curves of the silica cladding, 4.1 mol.% Ge-doped core, the effective mode index n_i of the guiding wavelengths, Cargille index-matching liquids, and the thermo-optic polymer OCK-433 (Nye Lubricants). The 4.1 mol.% Ge-doping concentrations approximate to the core of the SMF-28 (Corning) fiber. The refractive index difference Δn between the core and cladding is almost wavelength-independent and operating wavelengths are well-confined to propagate in core without LP_{01}-λ_c. The mode field diameter (MFD) expands when the wavelength increases and the refractive index goes down simultaneously. Accordingly, the $|dn/d\lambda|$ of the n_i is steeper than that of the core and cladding. While the dispersive optical materials are applied on the SPF, the evanescent wave tunneling becomes dispersive and the RID curves intersect with each other to generate LP_{01}-λ_c ascribing to material dispersion discrepancy [12]. When the cross angle between them is larger, the LP_{01}-λ_c becomes sharper and the resulting filter edge is steeper. The $|dn/d\lambda|$ in Fig. 2 are n_i > Ge-doped core > cladding > OCK-433 > Cargille liquids. Thus, the LP_{01}-λ_c is short-pass filter and the corresponding cross angle will be larger by using Cargille liquids. A sharp LP_{01}-λ_c not only achieves steeper filter edge but

also contributes to higher rejection efficiency for the stopband, which are the key factors to an efficient local ASE suppression in EDFRL.

In fabrication, the fiber short-pass filter is made from a SPF using SMF-28 fiber with dispersive polymer overlay [12]. A section jacket of the SMF-28 was removed and the naked fiber was then embedded in the silicon V-groove whose radius of curvature is 15 m and which was precision etched to make the central cladding thickness beneath the wafer surface of around 2.7 μm. The exposed cladding was polished away with the polishing slurry of grain size of around 100 nm until the strong evanescent wave can be accessible. The insertion loss, polarization dependent loss, effective index n_{eff}, and effective interaction length L_{eff} of the SPF at 1550 nm wavelength were then measured to be 0.26 dB, 0.09 dB, 1.449 and 11 mm through liquid-drop test and L-Z formula fitting [12]. The Cargille liquids and OCK-433 are isotropic mediums with no birefringence and were respectively applied on SPF with the thickness of around 1 mm while a TE-cooler (TEC) plate was placed on them with 0.1°C temperature resolution. The thermo-optic coefficient of OCK-433 is $-3.6 \times 10^{-4}/°C$ and thus the refractive index decreases with increasing temperature. A broadband light source (1250 ~ 1675 nm) containing multiple SuperLuminescent Diodes (SLDs) was launched into the SPF and the wavelength responses v.s. temperature variation were shown in Ref. [12]. For the wavelengths longer than the LP_{01}-λ_c, they suffered strong optical losses since the refractive index n_o of the dispersive material is higher than n_{eff} of the SPF. The rejection efficiency of the short-pass filter was above 50 dB for 11-mm-long L_{eff} (> 45 dB/cm) and the tuning range was of around 400 nm (1250 ~ 1650 nm) wavelength by temperature variation of 15°C (26.7 nm/°C) [12]. By incorporating the thermo-optically tunable short-pass filter into the resonant cavity to provide a wideband tunable loss window shown in Fig. 1 the EDFRL was fulfilled. The EDL001 (POFC) with the length of 20 meters is our available EDF and is designed for L-band amplification. The absorption coefficients are of around 12 dB/m and 30 dB/m for 1480 nm and 1530 nm wavelength, respectively. It was pumped by a 1480 nm diode laser with 220 mW launched power and absorbed the generated wavelengths in C-band to give amplification in L-band. The optical feedback was achieved by the 10% power splitting from a broadband tap coupler and the traveling-wave cavity made the ASE peak wavelength lasing. When the LP_{01}-λ_c was tuned, the unwanted ASE was suppressed and the lasing wavelength moved accordingly. The in-line isolator restricted the EDFRL to occur in only co-propagation direction of pump light with the isolation ratio of 35 dB from 1450 nm to 1650 nm wavelength.

3. Results of measurements

To investigate the influences of the sharpness of the LP_{01}-λ_c, the Cargille liquids were applied on SPF first and the pump laser was biased at current of 605 mA (optical power=140 mW). The spectral responses of the EDFRL are shown in Fig. 3 and the initial lasing wavelength without liquids is 1599.4 nm under 0.2 nm optical resolution of the optical spectrum analyzer. When the refractive indices 1.456 (n_D) and 1.458 (n_D) were used, the lasing wavelength moved to shorter wavelengths and the laser peak power decreased following the gain profile. The pump laser was re-biased at currents of 758 mA (175 mW) and 943 mA (205 mW) for curves 1.456 and 1.458, respectively, to attain gain saturation. Subsequently, the Cargille liquids were replaced by OCK-433 and the spectral responses are shown in Fig. 4 while the pump laser was biased and fixed at current of 1 A (220 mW) through the experiments. Before forming a ring cavity, the ASE peak wavelength for the 20 meters of EDL001 was measured to be 1596.6 nm. For EDFRL, the lasing wavelength when the OCK-433 was heated to 43°C to make all wavelengths passed was 1595.8 nm. The lasing wavelength (1595.8 nm) is not consistent to the initial lasing wavelength (1599.4 nm) of using the Cargille liquids due to the fusion splicing between the SMF-28 and EDL001. Their fiber structures are so different and thus the conditions of each splicing were not identical, which made the initial lasing wavelengths different. When the temperature of the TEC was cooling down, the lasing wavelengths were again moving toward shorter wavelengths and the peak power was

gradually reduced following the gain profile of the EDF. While the temperature was tuned to 39.6°C, the lasing wavelength was 1569.8 nm and was at the short wavelength edge of the ASE. Thus, the tuning range of the EDFRL is 26 nm by temperature variation of 3.4°C and the typical signal-ASE-ratio is above 40 dB.
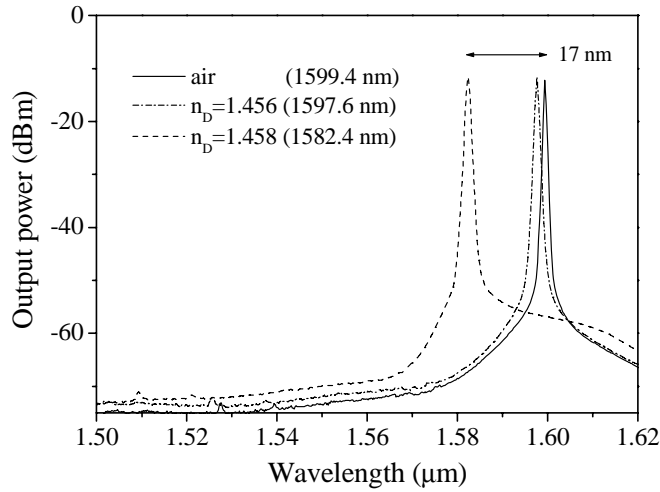

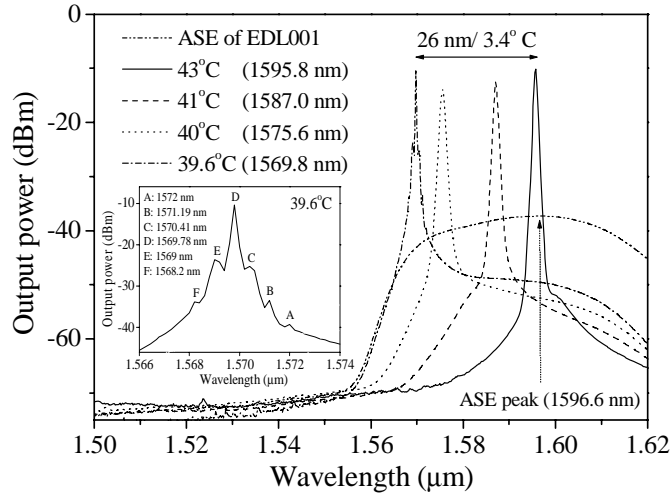Fig. 3. Spectral responses of the EDFRL using Cargille index liquids on SPF.

Fig. 4. Spectral responses of the wavelength tuning of the EDFRL when OCK-433 polymer was cooling down.

From Fig. 4, the ASE becomes conspicuous at 39.6°C since the ASE peak was at 1596.6 nm and thus the residual ASE were accumulated and propagated in fiber. The residual ASE can be eliminated if the short-pass filter was placed just right before the laser output. At 39.6°C, the inset plot in Fig. 4 shows the laser spectrum near the edge of the gain bandwidth and where the comb-like filtering phenomenon reflects the resonant coupling between the SPF and the top surface of the optical polymer, which occurs only when n_o is substantially higher than the n_{eff} [7]. The resonance spacing is around 0.79 nm and the resonant coupling can be eliminated by inducing roughness on top surface of the polymer or enhanced by improving the finesse to serve as a DWDM filter based on our SPFs with very long L_{eff}. In Fig. 3 and 4, the laser linewidth broadens and the wavelength-tuning efficiency increases when lasing

wavelength moves downward and the measurements of laser linewidth are listed in table I. The mean FWHM linewidth is around 0.5 nm, which means that the EDFRL is not under the single-longitudinal-mode operation because the tap coupler can not play as a high Q resonator, and the laser linewidth is related to the cross angle between RID curves. When the lasing wavelength moves downward, the laser linewidth broadens since the emission cross-sections of the erbium ions gradually decreases at short wavelengths, see ASE spectrum in Fig. 4. Although the gain profile inclines to gradually decrease at left-half part of the ASE, which is advantageous for the guided peak wavelength to strongly lase, the spectral curves, falling toward lower-right, of the short-pass filter will compensate the inclination [12]. Therefore the amplification for the guided peak wavelength is not as strong as before and the optical gain is robbed by adjacent wavelengths to induce linewidth broadening. As to the tuning efficiency, it was enhanced by similar reasons when lasing wavelength moved downward and is related to the sharpness of the cutoff. Actually, the guided peak wavelength is determined by the superposition of the overall emission cross-sections from the whole EDF and the suppression spectra of the local short-pass filter. For an ideal short-pass filter with an abruptly sharp LP_{01}-λ_c, the lasing wavelength will occur at the edge and moves with the tuning. However, the cutoff can not be very sharp for real short-pass filters and thus the lasing wavelength can occur at the long-wavelength side of the cutoff for high emission cross-section area. When the LP_{01}-λ_c moves downward to the lower emission cross-section area, the lasing wavelength can only occur at the edge of the cutoff. Tuning from high to low emission cross section area, the lasing wavelength moves faster than the LP_{01}-λ_c and thus the tuning efficiency grows up with decreasing temperature. The laser linewidth will be narrower by using the short-pass filter with sharp cutoff since the modes competitions will be highly reduced at wavelengths longer than the cutoff. From Table 1, the 30 dB linewidth is narrower by using the Cargille liquids than the OCK-433 because the former achieves steeper cutoff than the latter (see Fig. 2).

Table 1. Laser linewidth of the EDFRL

Cargille liquids				
Peak wavelength (nm)	1582.4	1597.6	1599.4	
FWHM (nm)	0.75	0.47	0.42	
30 dB (nm)	3.98	3.3	2.66	
OCK-433				
Peak wavelength (nm)	1569.8	1575.6	1587.0	1595.8
FWHM (nm)	0.12	0.8	0.6	0.52
30 dB (nm)	4.84	5.15	4.22	3.4

4. Conclusion

We have demonstrated a simple, high-efficiency and continuously tunable EDFRL based on an efficient local LP_{01}-λ_c using a novel wideband tunable fiber short-pass filter in ring resonator. The laser can be tuned close to the short-wavelength edge of the gain bandwidth and the tuning range is 26 nm by 3.4°C temperature variation with the signal-ASE-ratio of around 40 dB. The FWHM linewidth is about 0.5 nm and is related to the cross angle between RID curves. The short-pass filter provides widely thermo-optically tunable local ASE suppression with high rejection efficiency (> 45 dB/cm) for the wavelengths longer than the cutoff. Based on our investigation, a novel fiber with distributed LP_{01}-λ_c for tunable EDFAs covering S-, C-, and/or L-bands and tunable Raman amplifiers are promising and are now in progress. The single-longitudinal-mode operation for fiber lasers can be performed by exploiting a wideband high Q resonator, e.g. dielectric coating, in future works.